¹T. Srikanth

²Dr. A. S. Kannan

A Comparative Evaluation of Hybrid GEO-RBFNN and GBDT-BCMO Methods for Power Quality Improvement using

for Power Quality Improvement using Renewable Energy Resources in Distributed Generation



Abstract: - This research presents a hybrid strategy to improving power quality via the combination of distributed systems that use solar Photovoltaic (PV) and battery storage. The Golden Eagle Optimizer (GEO) and the Radial Basis Functional Neural Network (RBFNN) are both part of the suggested hybrid technique. This method is often referred to as GEO-RBFNN. Here, the RBFNN approach is used to train the inputs using the target reference power of the prior instantaneous energy sources and the present load needs. In order to provide the best control signal and keep the Hybrid Renewable Energy Sources (HRES) running, the suggested technique uses load fluctuation to determine the PI controller gain settings. In GBDT-BCMO, we aim to achieve the objectives mentioned before. Applying the BCMO approach improves the GBDT machine learning technology. Inputs used to train the GBDT technique include the goal reference power, the present time necessary load demand, and the instantaneous energy of available sources in the past. When making predictions, the GEO-RBFNN approach takes into account all possible fluctuations in system characteristics, including active and reactive power, DC voltage, and more. Consequently, the suggested GEO-RBFNN technique produces the specified line voltage for reactive power compensation while minimizing power system damping. After running the suggested technique on the MATLAB/Simulink environment, its performance is evaluated in comparison to other ways that are currently available. By generating line voltage and enhancing power system damping, the GBDT-BCMO system offers reactive power compensation.

Keywords: GBDT-BCMO, GEO-RBFNN, Renewable Energy, Hybrid, Power Quality

1. Introduction

There has been a lot of buzz about hybrid power systems that combine wind and photovoltaic (PV) electricity as a way to create a greener, more sustainable energy future. These setups make better use of renewable energy by combining the intermittent generating features of wind and solar resources. Problems with power quality arise, however, when such a wide variety of sources are integrated into the power system. A number of variables affect the efficiency and dependability of the power supply; they include reactive power balancing, harmonics, frequency regulation, and voltage stability. Increased energy output and less reliance on traditional fossil fuels are two of the many benefits of hybrid PV-wind power systems. However, power quality problems like voltage variations and frequency deviations may arise from these renewable sources due to their intrinsic unpredictability and intermittency. If we want hybrid systems to work reliably with the grid as it is, we need to solve these problems thoroughly.

Efficient energy utilization, environmental protection, voltage stabilization, power quality enhancement, and harmonic reduction have all seen heavy use of the FACTS in recent years [1, 2]. Reducing power loss, improving and conditioning power quality, and regulating power flow, voltage, reactive power compensation, transient with steady state, and improving voltage stability are all achieved via a series of procedures. Distributed generation (DG) and renewable energy sources primarily serve to increase the power of electronic grid devices, which in turn increases the reliability and safety of electric utility services.

Power generation using renewable energy sources, such as solar and micro-hydroelectric devices designed for use in micro grids [6]. Power electronic converters are the backbone of transmission and distribution/utilization systems, which in turn rely on RES [6]. Today, the power system is an integral part of Power Quality; it encompasses the whole power supply chain, from generation to transmission to distribution. Voltage dips, outages, surges, imbalances, and harmonics are all examples of power quality issues that may arise in the distribution system. Customers incur losses due to insufficient PQ. The control models and power electronics devices have

¹ Ph.D Research Scholar, Department of Electrical Engineering, Annamalai University, Chidambaram, Tamil Nadu, India, skanthmtech@gmail.com

²Associate Professor, Department of Electrical Engineering, FEAT, Annamalai University, Chidambaram, Tamil Nadu, India Copyright © JES 2024 on-line: journal.esrgroups.org

planned the voltage and power fluctuations. Users in the industrial, commercial, and residential sectors are dealing with a higher volume of PQ issues. FACTS devices have the potential to enhance the power quality of the power system linked to WF, including multi-models.

By reducing the incidence of line output, FACTS devices not only prevent failures but also minimise side effects and improve power system dependability. Reactive voltage and PF on the gearbox system are active in FACTS devices' higher voltage power electronics utilisations [4]. In order to enhance the FACTS, record in power systems, the substantial investigation is focused on novel VSC topologies, which are the outcome of enhancing the structure and power system security. The result is put into play in smart grids by FACTS devices, which are headed by RES [4].

There are many potential benefits to having renewable DGs in the distribution system. These include helping with voltage support, improving power quality, reducing loss, making the utility system more reliable, and delaying expenditures in transmission and distribution infrastructure upgrades or new construction [5]. But depending on the power converter technology and kinds of DG units, when the distribution generator is connected to a DS, it might cause harmonic propagation in the system. Two types of DG exist: those that use inverters and those that do not. Some examples of inverter-based DG include fuel cells, micro turbines, solar systems, and wind turbine generators; they all connect to the grid via power converters. Small hydro synchronous and induction generators are examples of distribution generating units that are not tied to inverters [6]. Installed at the level of the distribution system electric grid, the distribution generator is strategically placed close to the load centre. It is common practice to analyse DG's effects on voltage profile, power losses, harmonic distortion, dependability of the power system, and short circuit current separately. The optimum installation of DGs is the primary determinant of the advantages that may be derived from them.

The aim of this paper is a hybrid control system is suggested in this study as a means to enhance power quality in grid-integrated HRES. A hybrid control scheme combining GBDT and balancing-composite motion optimisation is called the GBDT-BCMO Technique. The suggested method is called GEO-RBFNN and is a wrapper for both the Golden Eagle Optimizer (GEO) and the Radial Basis Functional Neural Network (RBFNN). Using hybrid GBDT-BCMO and GEO-RBFNN methods, we evaluate the effectiveness of renewable energy systems in improving power quality.

2. Recent research work: a brief review

Prabhu, Mr. & K, Sundararaju [7] The use of solar energy in distributed generation systems (DGs) is a relatively recent development in the power industry. In order to meet the needs of the local community, these dispersed generation units work together to create a micro grid that transmits electricity to the utility grid. The use of solar energy resources for power electronics applications and the reduction of grid harmonics have gained global fame. Optimal numerical parameters for solar power generation - Unified Power Quality Conditioner (PV-UPQC) are achieved by the use of a Resilient Direct Unbalanced Control (RDUC) algorithm in this study, which improves the controller's performance. Next, the outcomes of the suggested RDUC algorithm for solar feed UPQC systems are examined using voltage sag, swell, and removal of current harmonics. Evaluators found that the suggested unified power quality conditioner removed distortions in the supply current and load voltage produced by nonlinear loads and the addition of fifth and seventh harmonics to the AC mains voltage. Under different operational circumstances, experiments are conducted to verify the accuracy of the Resilient Direct Unbalanced Control scheme's simulation results. The results of the tests demonstrate that the system performs well both in a steady state and under dynamic situations such load imbalance, insolation change, voltage sag, and swell. Lastly, the suggested optimization-based grid current and voltages were determined to have Total Harmonic Distortions (THDs) that were within the IEEE standard's limitations. Gitanjali Mehta and S. P. Singh [8] As a result of their lower environmental impact and increased efficiency in using existing resources, renewable energy sources (RES) are quickly becoming the preferred method of producing green electricity. Using a single-stage, three-phase renewable energy source (RES) distributed generating system that incorporates active power filter (APF) capability into the grid-interfacing inverter to perform many roles at once, this study covers the modelling, control, and design analysis of the system. The grid connection is made possible by connecting the RES to the DC side of the power source inverter. When the supply voltage is distorted, the inverter acts as a power converter, injecting

the power produced by the renewable energy sources (RES) into the Power Conversion Centre (PCC) and shunting the Active Power Factor correction (APF). This compensates for load current harmonics, reactive power demand, and imbalance. Either of these tasks may be completed alone or in tandem with the other. It follows that the developed controller may either act as an APF or manage the power flow between the grid and the RES. To confirm the operation and control concept, experiments are conducted using DSP and simulations are run in MATLAB.

Moorthy, et al [9] Optimal energy management for a hybrid electric vehicle system is suggested in this article using a new hybrid approach. We name the method we're suggesting WF2SLOA since it combines two algorithms: Kernel Wingsuit Flying Search and Sea Lion Optimisation Algorithm. The energy management system's use of the WF2SLOA approach primarily aims to distribute torque between the electric machine and the engine. Parametric study on many important elements, including state types and number of states, states and action discretization, exploration and exploitation, and learning experience selection, is carried out in this paper during the development of WF2SLOA-based energy management. In order to evaluate the performance of the suggested approach, it is used in conjunction with the current methods in MATLAB/Simulink. Consequently, the results show that reducing the vehicle's fuel usage is possible with the selection of the learning experience. In addition, the research on states and action discretization shows that boosting the states discretization has a negative effect on fuel consumption, whereas increasing the action discretization reduces it. The fuel efficiency is enhanced by maximising the count of states as well. So, compared to the current approaches, the simulation results demonstrate that the suggested strategy performs better. With the WF2SLOA technique, we get 1.5420 for the mean, 1.5043 for the median, and 0.0509 for the standard deviation.

Kumari, Naresh [10] This dissertation demonstrates the use of a remarkable hybrid strategy for effective energy management in grid-connected micro grids (MGs) using energy scheduling. This hybrid approach combines the RBFNN and BBMO techniques, which stand for Bumble Bees Mating Optimisation and Radial Basis Neural Function Network, respectively. The MG system is comprised of solar, wind turbine, micro turbine, and battery storage components. Here, batteries are used to keep the output power consistent and steady. Using the RBFNN approach, the grid-connected MG scheme's essential load demand is continuously monitored. BBMO plans the optimal mix of MG by considering the anticipated load demand. Adopting a two-pronged approach to managing MG's energy use helps mitigate the effects of inaccurate predictions of renewable power generation. First, to reduce power expenses, MG may be programmed to use a variety of renewable energy sources (RESs). The second method involves reducing predicting errors and balancing power flows from the planned energy reference using the summarised rule. Limitations include availability of renewable energy sources, electricity, and charging modules. In order to determine which approach is superior, we compare it to two existing ones, such as the Genetic Algorithm and the Cuttlefish Algorithm.

Vanitha, V. & Vallimurugan, E. [11] The expansion of the internet of things (IoT) has made it essential to efficiently manage energy in order to satisfy the increased demand, which is caused by the integration of a significant number of smart devices in residential buildings. Hence, this study suggests a smart approach to energy management for residential structures that are facilitated by the Internet of Things (IoT) by using the hybrid Gradient Boosting Decision Tree -Artificial Transgender Longicorn Algorithm (GBDT-ALTA). The suggested method primarily aims to lower the Peak-to-Average Ratio (PAR) by reducing the customer's power cost. The waiting time threshold is used in the suggested method as a result of the scheduling procedure of home electric devices. In this context, we will examine three distinct kinds of electrical appliances: those that are shiftable, those that are thermostatically regulated, and those that are operated in a more generalised fashion. The processing of scheduling for shiftable electrical equipment is connected to real-time pricing signals (RTPS) in utilities. The goal of the GBDT-ATLA approach is to minimise costs while minimising unacceptable waiting times by taking into account the trade-off between power cost and waiting time. The suggested method also keeps the grid stable, which is important since the PAR is what makes the grid stable. Simulation results show that the GBDT-ATLA approach outperforms existing methods such as Slime Mould Optimisation (SMO), Chaos Game Optimisation Algorithm (CGO), and Side-Blotched Lizard Optimisation Algorithm (SBLO) when the proposed method is implemented in the MATLAB/Simulink site. The suggested method achieves efficiencies of 99.7300%, 99.6513%, 99.8363%, and 99.7916% under 100, 200, 500, and 1000 trials, correspondingly.

2.1. Background of research work

Improving renewable energy systems' Power Quality (PQ) has been proposed in a number of ways. The quantity of compensations offered by the inverter is entirely dependent on the availability of the obvious power rating, which is the fundamental downside of using grid-interactive inverters. Consequently, to alleviate the PQ problems, an extra PQ compensator with a solid controller might be set up. As a PQ conditioner, distribution static compensator (DSTATCOM) in conjunction with grid-interactive inverters mitigates current-based PQ problems, mitigating one of the drawbacks. The IBatMFOA control strategy unites the Improved Bat Algorithm (IBat) with the Moth Flame Optimisation Algorithm (MFOA), nevertheless, there may be computational difficulties associated with integrating several optimisation techniques. Another approach uses an Adaptive Neuro-Fuzzy controller in conjunction with a PV-UPQC system; this shows better performance under different load situations, but it is difficult to deploy due to the complexity of the controller's design and tuning. The number of compensations provided by grid-interactive inverters is entirely dependent on the availability of the apparent power rating. Consequently, to alleviate the PQ problems, an extra PQ compensator with a solid controller might be set up. As a PQ conditioner, distribution static compensator (DSTATCOM) in conjunction with grid-interactive inverters mitigates current-based PQ problems, mitigating one of the drawbacks. When assessing the system's performance under changing dynamic circumstances, the regulation of the dc-link voltage is also crucial. The dclink voltage controller has to respond quickly in order to get the de-link voltage back to its reference value when the system is dynamic. To modify DSTATCOM's dc-link voltage, the standard PI controllers are used.

3. System design of power quality with distribution generation

An integral part of distribution generation (DG), the voltage source inverter links renewable energy sources (RES) to the power grid and supplies the generated electricity [12]. In a nutshell, the RES generates electricity at the lowest possible DC voltage, whereas the WT generates electricity at varying rates and AC voltages. Power modifications are necessary before connecting to DC-link for RES. By lowering the error target function, BCMO enhances GBDT's machine learning approach. The rectifier attached to the DC-link most likely makes the RES a DC or AC source inverter. The PVDG system with integrated PQ enhancement capability (PQE) is shown in Figure 1. A capacitor (CPV) connected to the solar array allows the boost converter to regulate the voltage of the array in order to maximise power extraction using a maximum power point tracking method. Use the perturbation and observation (P&O) paradigm to achieve maximum power point tracking control. A direct current connection capacitor (Cdc) has been used to connect the boost converter to the PV inverter. In order to ensure that the solar inverter's ac side receives full power, the external voltage control circuit of the dc-ac inverter maintains a steady voltage across the Cdc. Notable in PVDG is the photovoltaic inverter, which facilitates the connection of the solar module to the grid and, thereafter, generates electricity with improved power quality characteristics. Two controllers—a load current analyzer (iL) that determines the active power, reactive power, and harmonic components needed by the load, and a DC voltage controller that keeps the solar inverter at a constant DC voltage—perform the aforementioned duties of the photovoltaic inverter. The inverter and reference inverter current estimator (iref) units work together.

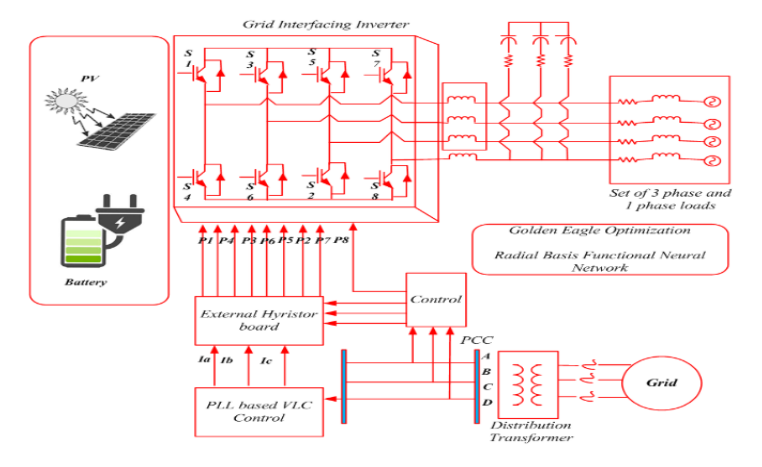


Figure 1: Distribution Generation Schematic for RES-Enhancing Power Quality

3.1 Distribution generation (DG) model

The DG connects the generating and transmission systems in the power system to the consumer load [13]. The electricity distribution services make use of them since they are inexpensive to install and have a straightforward design. Be sure to check the impact of the power system's output on a regular basis in the distribution network to prevent power interference. We show the DG's dependability based on the environment, system setup, the number of installed loads, and the location of each load. All or part of the loads are supplied by the renewable DG unit, depending on the setup.

3.2. Problem derivation of PV

In order to produce the required amount of output electricity, the photovoltaic system employs a multitude of solar panels [14]. The photovoltaic cell's mathematical characteristics are described as,

$$i = i_{PV,cell} - i_{o,cell} \left[E \left(\frac{V + i \, rs}{AV_t} \right) - 1 \right] - \left(\frac{v + i \, rs}{r_p} \right)$$
(1)

The variables that make up a photovoltaic cell are its current (iPV,cell), its saturation (io,cell), its thermal voltage (io,cell), the electron charge (q), the Boltzmann constant (k), temperature (t), and the constant ideality diode (A).

3.3 Mathematical model of battery system

Taken into account are the battery's charge status, capacity, and time usage. A battery system parameter table.

$$at(t) = at(t-1) * (1-\sigma) + \left[f_g - \frac{fd_l}{f_{inv}} \right] f_{bc}$$
(2)

There is an hourly self-discharge rate denoted by σ and a battery bank discharging rate denoted as η bf.

3.4 System Controller for Grid-Tie PV Inverter

The suggested 1ϕ PV inverter along the EPQ function is shown in Figure 2. The AC side of the inverter circuit is responsible for causing the output terminal voltage to be Vinv. Each state of the switch, T ii = 1, 2, 3, 4, has two possible values: "1" when the switch is open and "0" when it is off. That is why P has two distinct values, 1 and 1, when the output voltage of a solar inverter is -vdc and vdc. The function P is substituted by a continuous switch operation S \in -[1,1] in order to get a linear model of a solar inverter. Hence, the following two equations outline the dynamic behavior of PVDG:

$$l_{Inv} \frac{DI_{Inv}}{dt} = s.V_{DC} - rI_{Inv} - V_G$$
(3)

$$C_{DC} \frac{DV_{DC}}{dt} = I_{Inv} - s.I_{Inv}$$
(4)

When it comes to controlling the grid-connected inverter at PVDG, there are two loops that are linked in series. One loop regulates the current flowing into the power supply, while the other loop controls the voltage coming from the outside. In response to PQ-related complexity, the current loop safeguards the current. Therefore, current drivers must include harmonic features, such as reactive power adjustment. To maintain a steady flow of electricity on PVDG, the direct current connection voltage controller is designed.

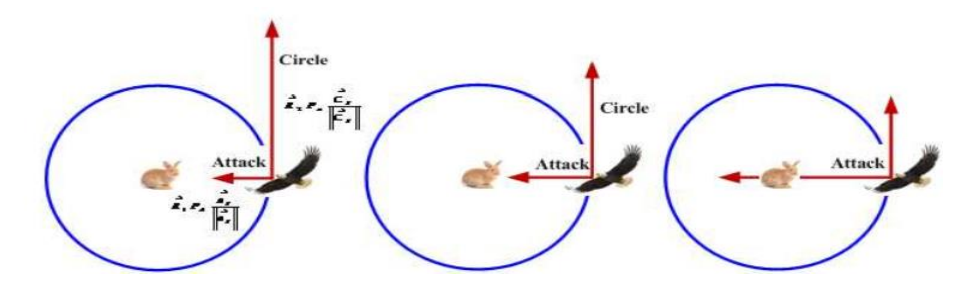


Figure 2: GEO go from an aggressively exploring (intense cruising) to an aggressively attacking (exploitative) state of mind.

4. Proposed Methods Using Hybrid Approach

4.1 Gradient Boosting Decision Tree and Balancing Composite Motion Optimisation (GBDT-BCMO)

By integrating reactive power and grid current harmonics correction and systems into its control method, the goal of the study is to maximise the performance of the grid-tie photovoltaic inverter. Distribution generation (DG) systems will be able to regulate the PV inverter to do numerous tasks, such as (i) compensating for reactive power and (ii) active power flow regulation between the grid and the PV inverter. The aforementioned goals are the basis for GBDTBCMO's design and implementation. Machine learning's GBDT solves classification and regression issues by creating a set of end trees that serve as forecast models—basically, weak forecast models. The GBDT-BCMO method of control generates the PI controller gain parameter in response to changes in the load in order to achieve the highest possible control signal and regulate the energy consumption of the HRES. The suggested method's prediction procedure handles all kinds of changes to system characteristics, such as dc voltage, real and reactive power, and others. Therefore, in order to control line voltage and dampen the power system, the GBDT-BCMO approach will enhance the accomplishment of reactive power compensation. The GBDT-BCMO method's process steps is shown Figure 3.

4.2 Golden Eagle Optimization and Radial basis Functional Neural Network (GEO-RBFNN)

The GEO-RBFNN technique is the suggested approach since it combines GEO and RBFNN. At its heart, GEO is GE intelligence, which it uses to fine-tune its spiral route for hunting at different speeds. An artificial neural network (NN) known as radial basis function neural network (RBFNN) uses mathematical model fields as activation functions. Here, the parameters for the arrival charge jobs are approximated using analytic probability distributions. Then, the sizing issue is dealt with using mixed-integer optimisation. Several time windows after the EV's arrival time are reserved for charging under the GEO-RBFNN approach. Even while the charging station gets to choose when the electric car begins charging, it can't stop it once it starts. The GEO-RBFNN approach improves the scalability of the optimal sizing technique. The GEO-RBFNN method's process steps is shown Figure 4.

GBDT-BCMO Steps

Step 1: This stage introduces the acknowledged basic learner h(x). Where xn = (x1i; x2i; ...xpi) is the total number of anticipated variables and yi is the prediction label. Interior fault stator current (C) is the input to the current GBDT technique.

$$f_0(x) = Arg \; M_{\beta}^{in} \sum_{i=1}^{N} l(y_i, \varphi)$$
 (5)



Step 2: Accuracy calculations for each categorization provide the basis of this step's evaluation of the function's primary goal. The calculation for accuracy is,

$$accuracy (\%) = \frac{TP + TN}{TP + FN + FP + TN} \times 100$$
(6)

This is where the count of accurate and incorrect predictions, represented by TP and TN, FN and FP, respectively, are recorded for an actual class



Step 3: we find the direction of the gradient of the residuals for m = 1: M by computing

$$Y_i^* = -\left[\frac{\partial l(y_i, f(x_i))}{\partial f(x_i)}\right]_{F(x) - F_{m-1}(x)} \quad i = \{1, 2, \dots, n\}$$
 (7)



Step 4: We evaluate the basic classifiers to get the first model and fit it to the data. The model h(xi; am) is fixed and the parameter am is evaluated using the least square approach.

$$A_{m} = Arg \underset{\alpha,\beta}{Min} \sum_{i=1}^{N} \left[y_{i}^{*} - \varphi h(x_{i}; A) \right]^{2}$$
 (8)



Step 5: The loss function is reduced after evaluating the current sample weight.

$$\varphi_m = Arg \ \underset{\alpha,\beta}{Min} \ \sum_{i=1}^N l(y_i, F_{m-1}(x) + \varphi h(x_i; A))$$



Step 6: Based on the following equation, the BCMO system is updated:

$$f_m(x) = f_{m-1}(x) + \varphi_m H(x_i; A)_{(10)}$$



Step 7: In the population, we estimate the values of the objective functions of individuals.



Step 8: Use the values of the objective function to determine how to rank the people.



Step 9: Termination

Figure 3: GBDT-BCMO Steps

GEO-RBFNN Steps

Step 1: Optimal performance of the golden eagle depends on the spiral motion of the GE. Every GE remembers the best spot ever, as said before. While cruising for the greatest meal, the eagle simultaneously assaults its victim.



Step 2: Choosing prey: In each cycle, the golden eagle chooses its prey and attacks it while cruising. One of the best solutions ever found by combining GE approaches with GEO is the prey model. The best solution that has ever been discovered can be memorised by the GE. The search agent selects its victim each cycle using flock memory. For each GE in a cruise with attacks, the relation of the chosen prey is used to calculate the vector. The revised location in memory is larger than the previous position. A crucial part of golden eagle optimisation is the prey choosing process. Depending on the GE prey, the selection process could be happen in its own memory.



Step 3: A vector starting from GE's present position and ending at the prey eagle's memory location structures the assault (exploitation). Equation (11) describes the attack vector (AV) of the golden eagle I.

$$a_1 = \overrightarrow{x_F}^* - \overrightarrow{x_I}_{(11)}$$



Step 4: Exploration during a voyage: determining the cruise vector (CV) from the assault vector (AV). The vector CV is perpendicular to the AV and forms a circle around it. It is believed that the hunter's linear speed is proportional to the prey's speed. The hyperplane's tangent contains the n-dimensional cruise vector. In order to calculate the CV, the n-dimensional cruise vector is situated within the hyper plane of the tangent. The equation is first computed in the hyperplane of the tangent. Another way to calculate hyper planes in n-dimensions is to use a vector that is perpendicular to the hyper plane and the hyper plane itself; this vector is called the normal vector of the hyper plane. Equation (12) shows that the scalar in the n-dimensional space is derived from the hyper equation.

$$H_1X_1 + H_2X_2 + \dots + H_NX_N = D \Rightarrow \sum_{J=1}^N H_JX_J = D$$
(12)

Where, ??? ? =[h1,h2,...,h?] specifies normal vector, ??:=[?1,?2,...,???] is variables vector, ??? ? =[?1,72,...,???] is the arbitrary point of ??=???? ? and hyper plane,???? = Σ h?????! Trepresents the CV of GE ??at iteration ??and is given in Equation (13). Let C??? be the position of the eagle ??as an arbitrary point on the hyper plane, and ???? ??be the normal hyper plane.

$$\sum_{J=1}^{N} A_J X_J = \sum_{J=1}^{N} A_J^T X_J^*$$
(13)



Step 5: Transfer to the new sites: Dislocation of the golden eagle includes both the vector and the assault. At iteration t, the vector representing GE I is given by equation (14).

$$\Delta X_{I} = \overrightarrow{R_{1}} P_{A} \frac{\overrightarrow{a_{I}}}{\left\|\overrightarrow{a_{I}}\right\|} + \overrightarrow{R_{2}} P_{c} \frac{\overrightarrow{C_{I}}}{\left\|\overrightarrow{C_{I}}\right\|}_{(14)}$$

The attack coefficient of iteration t is denoted by p???, and the t iteration is transformed into the golden eagles by the change in the cruise coefficient, which impacts the attack. These elements reside in the interval [0,1] and make up the random vector ??? 1, ??? 2. We shall talk about PC and PA later on. In equation (15), they are also computed.

$$\|\vec{a}_I\| = \sqrt{\sum_{J=1}^N A_J^2}, \|\vec{C}_I\| = \sqrt{\sum_{j=1}^N 1c_J^2}$$
(15)



Step 6: Switching gears from exploration to exploitation: In the prior approach, the golden eagle method exhibited the greatest propensity to travel during the initial phase of the hunting flight. Subsequently, it exhibited the highest propensity to attack the end states, which were associated with both high exploration during initial iterations and high exploitation during iterations when the optimizer was used.

Figure 4: GEO-RBFNN Steps

4.3 Tool for the modelling and simulation

Our study's suggested system was modelled and simulated using MATLAB/Simulink, a sophisticated tool. Due to its capabilities in building, modelling, and analysing dynamic systems, MATLAB/Simulink is the ideal choice for our research objectives. To begin the modelling process, we used Simulink's user-friendly graphical user interface to create a block diagram depicting the system's components and their interactions. In order to estimate and optimise the model parameters using experimental data, the optimisation toolbox in MATLAB was used. We were able to verify that our model was faithful to the dynamics of the actual system because of this. We were also able to conduct a thorough evaluation of its performance thanks to Simulink's simulation features, which allowed us to track its transient and steady-state behavior under various situations and inputs. The Simulink models were checked for accuracy by comparing them to real-world data and seeing how they performed. We also ran sensitivity analysis to see how changing important model parameters affected the final product. Our system model was developed, refined, and validated using MATLAB's flexible and efficient platform, making it an invaluable tool for accomplishing the study objectives.

5. Results and Discussions

Here we review the findings of the simulations and talk about how to get the best power quality improvement on grid-connected HRES systems. By optimising the grid-connected HRES system using the GEO-RBFNN approach, power quality is enhanced. Here, we evaluate the results of the simulations for grid-linked HRES systems in terms of optimum power quality development. One grid-connected HRES method that works with the GBDTBCMO system is power quality enhancement. The suggested solution is being tested experimentally on grid-linked HRES systems using the MATLAB environment.

5.1.1 Comparison of both Power quality improvement GEO-RBFNN and GBDT-BCMO approaches

Case 1: Change in Irradiance

In this scenario, the Irradiance decreases from 1000W per square meter to 800W per square meter between 0.2 and 0.3 seconds. After that, it remains constant at 1000 W/m² until the process is finished, as illustrated in Figure 5.

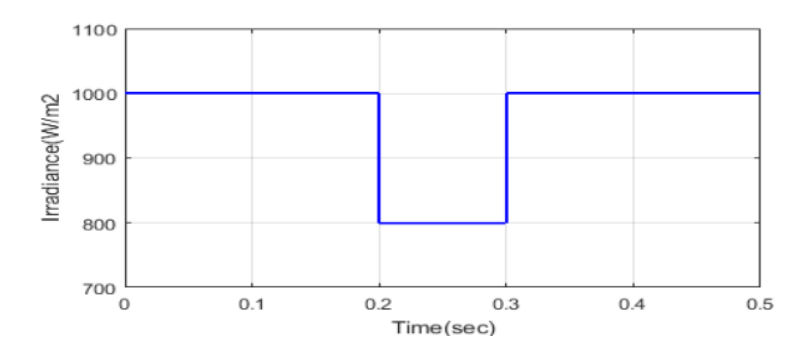


Figure 5: Irradiance versus time

In Figure 6, we compare the performance of DC link voltage between the proposed method, GEORBFNN, and existing methods. GEORBFNN achieves a voltage range from 0 to 22.4 V as the irradiance changes from 0.2 to 0.3 seconds. The existing techniques, GBDTBCMO, BCMO, ALO, and BAT, have voltage ranges of 0 to 22.1 V, 0 to 22 V, 0 to 21.8 V, and 0 to 21.6 V respectively. It's noteworthy that the proposed GEORBFNN method shows the highest voltage range among all techniques..

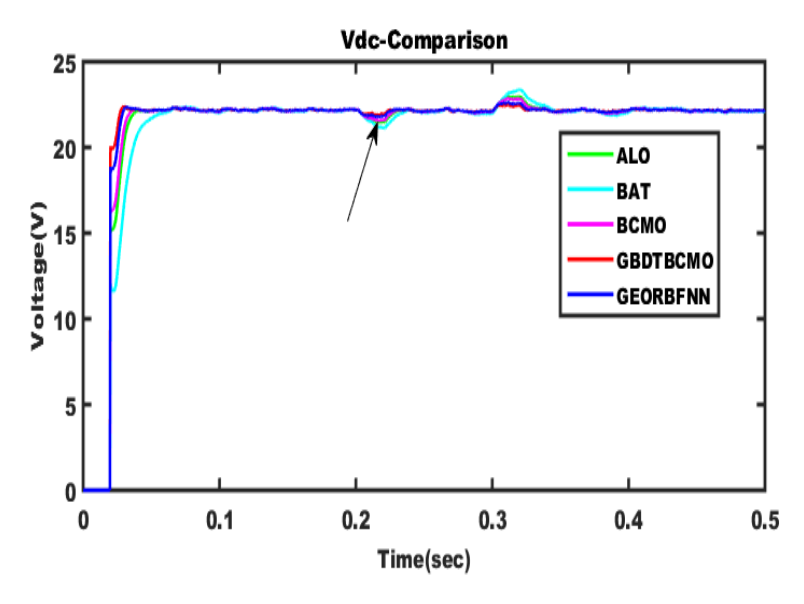


Figure 6: DC voltage Comparison GEORBFNN with existing strategies

Figure 7 illustrates a comparison of PV power analysis between the proposed and current strategies. In the proposed GEORBFNN method, the PV power reaches 6000 watts at 0.2 seconds, then decreases to 4000 watts by 0.22 seconds, before rising back to 6000 watts at 0.32 seconds. This 6000-watt range is then maintained throughout the method. On the other hand, in the GBDTBCMO method, the PV output initially reaches 5900 watts at 0.2 seconds, drops to 3800 watts by 0.23 seconds, then rebounds to 5900 watts by 0.33 seconds, maintaining this level until completion. In the BCMO approach, the PV output starts from 0 and climbs to 5870 watts by 0.2 seconds, before dipping to 3720 watts at 0.33 seconds, and then rising back to 5870 watts by 0.5 seconds, maintaining this level until the end of the process. Similarly, in the ALO method, the PV power starts at 0 and climbs steadily to 5850 watts by 0.2 seconds, then drops to 3700 watts by 0.33 seconds, and climbs back to 5850 watts by 0.5 seconds, holding this level until completion.

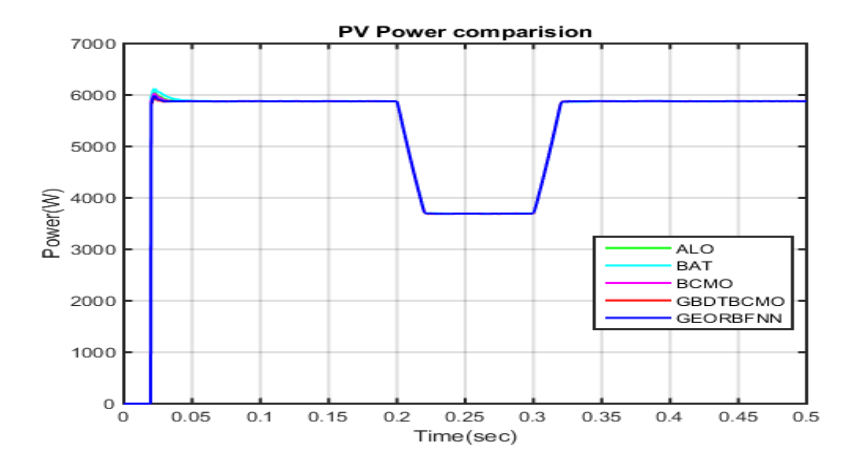


Figure 7: PV power analysis of the proposed and existing strategies

Figure 8 compares the proposed and existing methodologies for battery power analysis. The suggested GEORBFNN technique's power flows from 0 to 2300W and remains steady for 0.21 sec, then slightly reduces to 2280W for 0.32 sec before increasing to 2300W and remaining constant for 0.5 sec. The GBDTBCMO technique's power flows from 0 to 2320W and remains steady for 0.22 seconds, then slightly decreases to 2280W for 0.33 seconds before increasing to 2300W and remaining constant for 0.5 seconds. The BCMO technique's power flows from 0 to 2270W and remains steady for 0.22 seconds, then drops to 2250W for 0.33 seconds before increasing to 2270W and remaining constant for 0.5 seconds. The ALO technique's power flows from 0 to 2270W and remains constant for 0.22 seconds, then drops to 2250W for 0.33 seconds before increasing to 2270W and

remaining constant for 0.5 seconds. The BAT technique power flows from 0 to 2260W and remains constant up to 0.22 sec, then it decreases to 2250W at 0.33 sec, then increases to 2260W and remains constant up to 0.5secs.

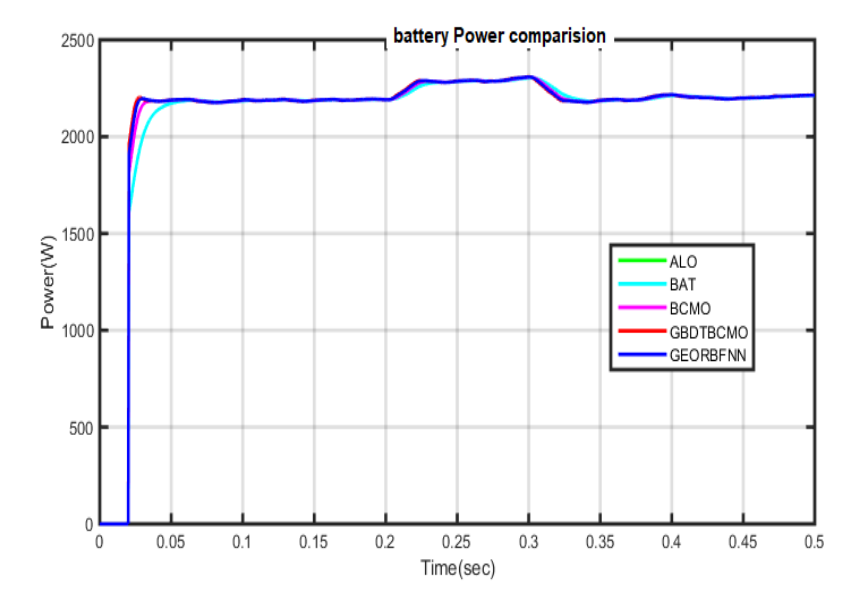


Figure 8: Battery power analysis of the proposed and existing strategies

Figure 9 compares the power usage of the proposed system and the existing system using different methods. The proposed GEORBFNN method starts at 0W and gradually increases to 1200W over 0.22 seconds, then drops to 1180W for 0.23 seconds before going back up to 1200W for 0.5 seconds. On the other hand, the GBDTBCMO method begins at 0W and increases to 1200W over 0.22 seconds, then drops to 1175W for 0.23 seconds before rising to 1190W for 0.5 seconds. The BCMO method starts at 0W and remains constant for 0.22 seconds, then drops to 1170W at 0.23 seconds before rising to 1180W and staying constant until 0.5 seconds. The ALO technique maintains a continuous power flow from 0 to 1180W for the first 0.22 seconds, then drops to 1150W for the next 0.23 seconds before going back up to 1180W for the last 0.5 seconds. Lastly, the BAT technique starts at 1180W, remains constant for 0.22 seconds, drops to 1130W for 0.22 seconds, then rises back up to 1180W and remains constant for 0.5 seconds.

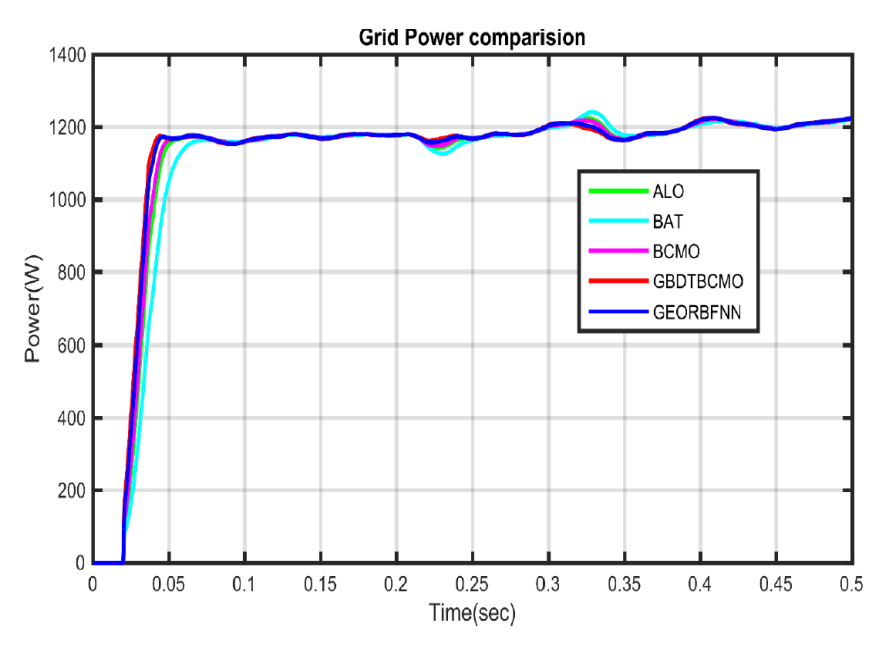


Figure 9: Grid power analysis of the proposed and existing strategies

Figure 10 displays a comparison of the total power for different techniques - GEORBFNN, GBDTBCMO, BCMO, ALO, and BAT - in both the proposed and existing systems. For the GEORBFNN technique, the power starts at 0

and rises to 9800W, staying constant until 0.22 sec. It then drops slightly to 7250W at 0.23 sec before increasing back to 9800W and remaining constant until 0.5 sec. Similarly, the GBDTBCMO technique sees the power start at 0 and reach 9750W, remaining constant until 0.22 sec. It then decreases slightly to 7150W at 0.23 sec before rising back to 9750W and staying constant until 0.5 sec. For the BCMO technique, the power begins at 0 and reaches 9700W, staying constant until 0.22 sec. It then decreases to 7140W at 0.23 sec before increasing back to 9700W and remaining constant until 0.5 sec. Likewise, the ALO technique starts at 0 and reaches 9700W, remaining constant until 0.22 sec. It then decreases to 7130W at 0.23 sec before increasing back to 9700W and staying constant until 0.5 sec. Lastly, the BAT technique's power flow also begins at 0 and reaches 9700W, remaining constant until 0.22 sec the power decreased to 7100W in 0.23 seconds, then increased to 9700W and stayed constant for 0.5 seconds

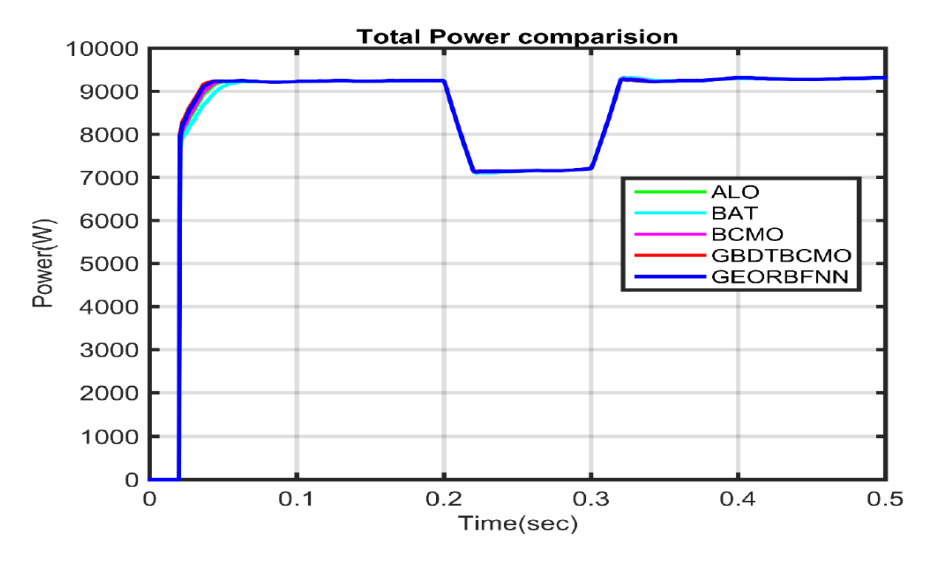


Figure 10 Total power analysis of the proposed and existing strategies

Case 2: Analysis of load fault

GEO-RBFNN

Figure 11 shows the results of the study on changes in irradiance. Throughout the entire procedure, the irradiance remains constant at 1000 W/m2.

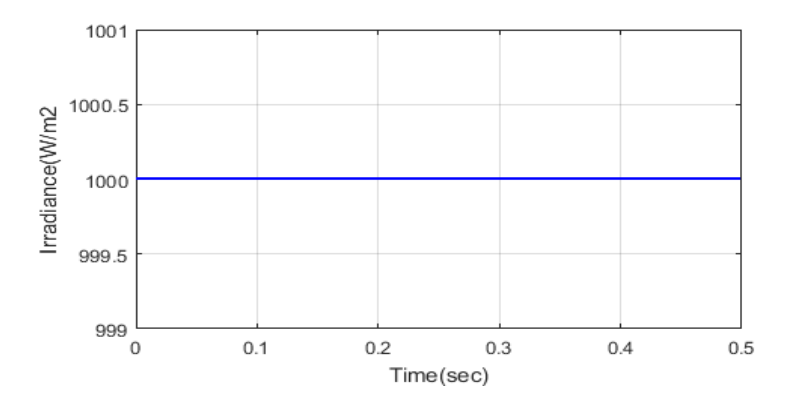


Figure 11 Performance analysis of Irradiance Change

In Figure 12, the comparison of DC link voltage performance between the proposed method GEORBFNN and existing approaches is shown. The GEORBFNN method results in a voltage range of 0 to 22.2 V when the irradiance changes from 0 to 0.5 seconds. On the other hand, existing techniques such as GBDTBCMO, BCMO, ALO, and BAT have voltage ranges of 0 to 22.1 V, 0 to 22 V, 0 to 22 V, and 0 to 22 V respectively. It is evident that the proposed GEORBFNN method achieves the highest voltage range compared to the existing techniques.

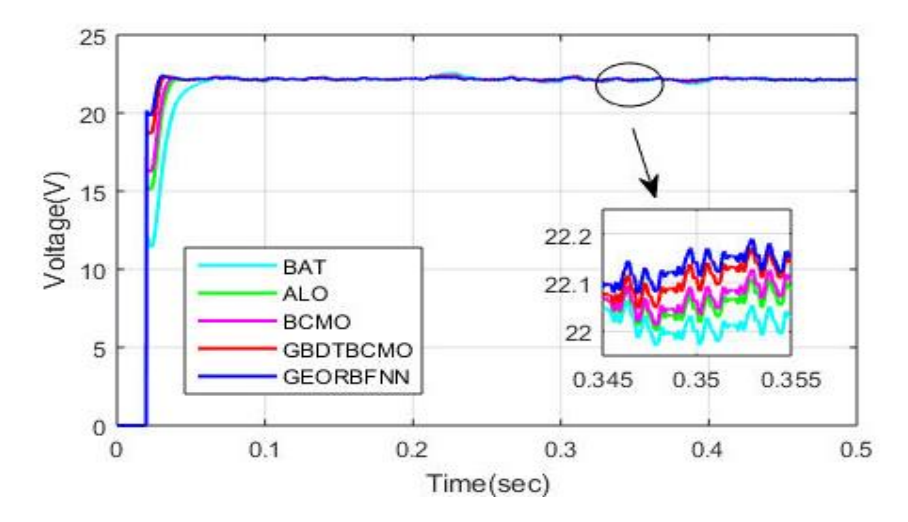


Figure 12: DC voltage Comparison GEORBFNN with existing strategies

Figure 13 displays a comparison analysis of photovoltaic power between the proposed and existing systems. In the proposed GEORBFNN technique, the PV power starts at 6000W from 0 to 0.015 sec, then decreases to 5900W at 0.26 sec and remains constant thereafter. In the GBDTBCMO technique, PV power reaches 6000W from 0 to 0.016 sec, then drops to 5880W at 0.27 sec, maintaining that level until the end. The BCMO technique sees power rise to 6000W before stabilizing at that level until 0.25 sec, dropping to 5879W at 0.26 sec, and staying constant until 0.5 sec. Similarly, the ALO technique and BAT technique both reach 6000W and then follow a similar pattern where the power remains constant until a slight reduction around 0.26-0.28 sec, holding steady thereafter until 0.5 sec.

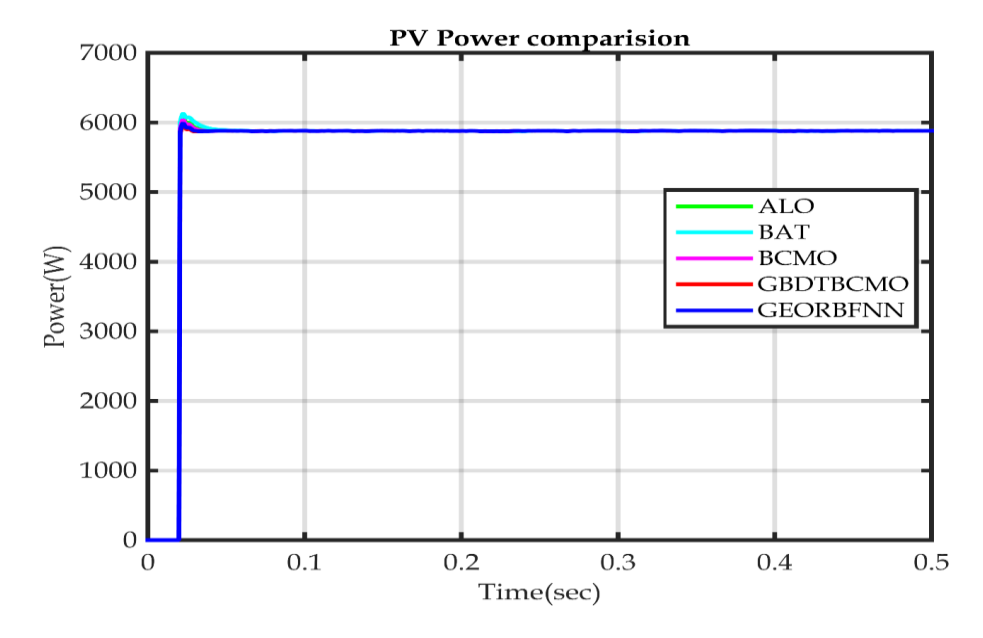


Figure 13: PV power analysis of the proposed and existing strategies

The graph in Figure 14 compares the power generated by different techniques for battery. The GEORBFNN technique starts at 0W and reaches 2350W, staying constant until 0.22 seconds before slightly dropping to 2190W at 0.25 seconds, then remaining constant until 0.5 seconds. The GBDTBCMO technique starts at 0W and reaches 2250W, staying constant until 0.23 seconds before slightly dropping to 2180W at 0.24 seconds, then remaining constant until 0.5 seconds. The BCMO technique starts at 0W and reaches 2200W, remaining constant until 0.23 seconds before dropping to 2165W at 0.24 seconds, then remaining constant until 0.5 seconds. The ALO technique starts at 0W and reaches 2200W, remaining constant until 0.23 seconds before dropping to 2165W at 0.24 seconds,

then remaining constant until 0.5 seconds. The BAT technique starts at 0W and reaches 2200W, remaining constant until 0.23 seconds before dropping to 2160W at 0.24 seconds, then remaining constant until 0.5 seconds.

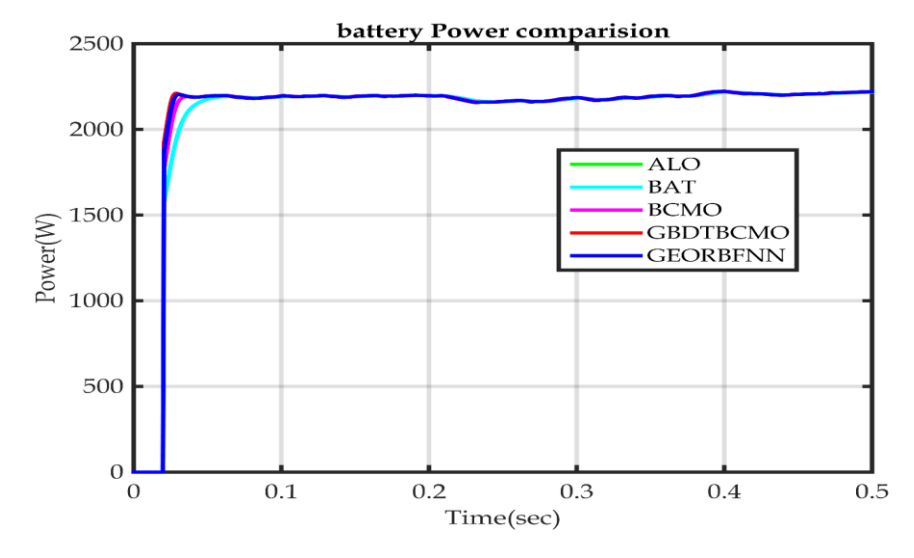


Figure 14: Battery power analysis of the proposed and existing strategies

Figure 15 illustrates a comparison of grid power between the proposed and existing systems. The power flow using the proposed GEORBFNN method initiates at 0W and remains constant for 0.21 seconds before decreasing to 1180W over 0.25 seconds, maintaining this level for 0.5 seconds. On the other hand, the GBDTBCMO method maintains a continuous power flow of 1200W for the first 22 milliseconds, drops to 1185W for the next 24 milliseconds, and remains stable for another 0.5 seconds. Using the BCMO approach, the power flows from 0 to 1190W, stays constant until 0.22 seconds, then drops to 1185W over 0.25 seconds, remaining steady for another 0.5 seconds. Similarly, utilizing the ALO method, the power flows from 0 to 1190W, remains stable until 0.22 seconds, and then decreases to 1185W over 0.24 seconds, staying constant until 0.5 seconds. The power flow using the BAT method starts at 0W and stays constant at 1175W for up to 0.22 seconds. It then drops to 1175W at 0.24 seconds and remains steady for 0.5 seconds.

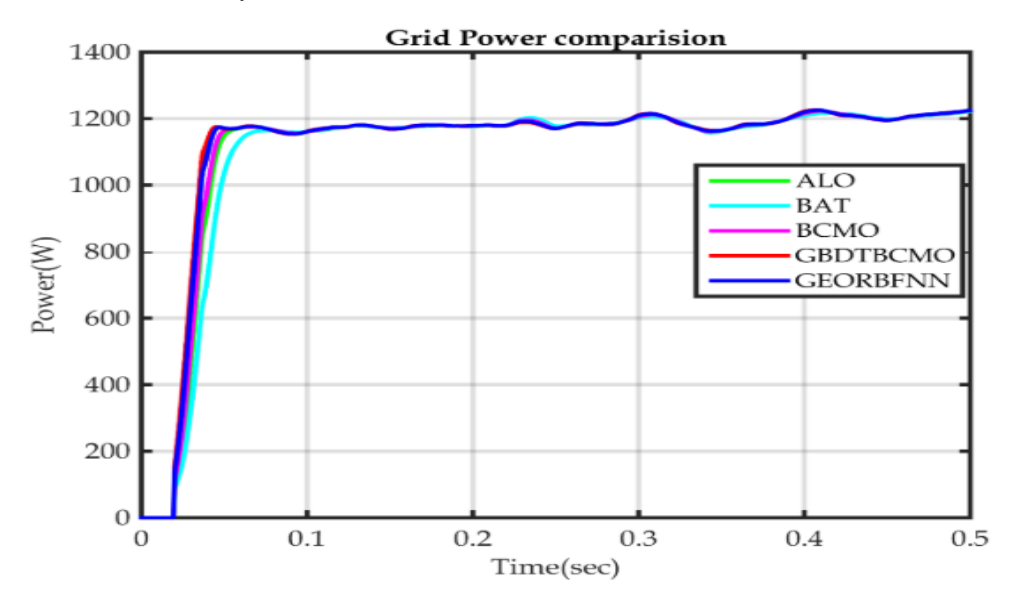


Figure 15: Grid power analysis of the proposed and existing strategies

Figure 16 displays a comparison of power between the proposed and existing systems. In the GEORBFNN method, power flows steadily from 0 to 9600W until 0.25 seconds, then decreases to 9360W and remains constant for half a second. On the other hand, the GBDTBCMO approach maintains a continuous power flow from 0 to 9500W for the first 0.24 seconds, then drops to 9240W for the next 0.25 seconds, and stays at that level for half a

second. The BCMO method starts at 0W and remains constant until 0.24 seconds, then decreases to 9230W within 0.25 seconds and remains constant for 0.5 seconds. The ALO method also starts at 0W and stays at 9500W for 0.24 seconds, then drops to 9230W for 0.25 seconds, and remains constant for 0.5 seconds. Lastly, the BAT technique's power flow reaches 9500W up to 0.24 seconds, then drops to 9210W at 0.25 second and stays constant until 0.5 seconds.

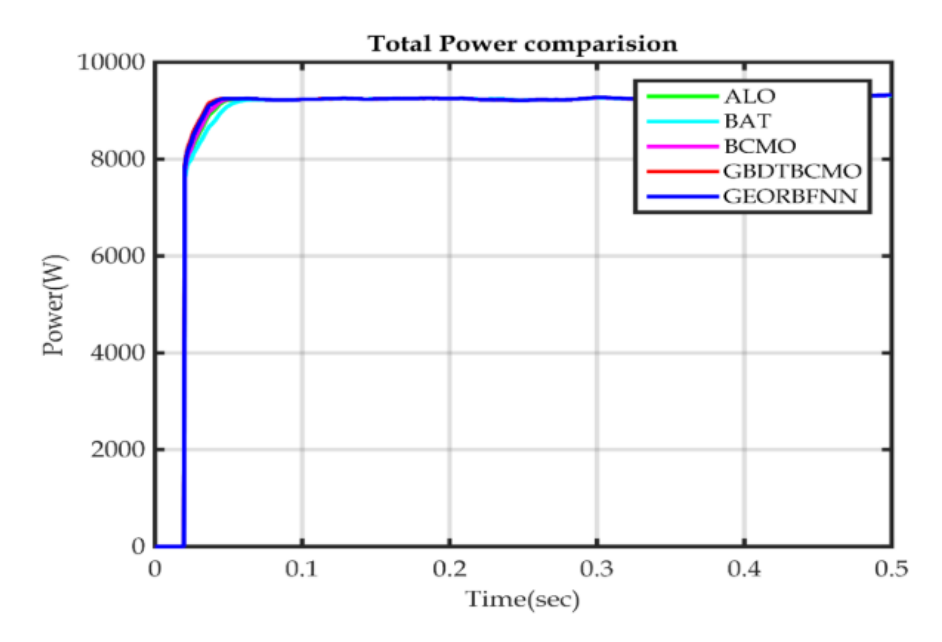


Figure 16: Total power analysis of the proposed and existing strategies

5.1.2 Voltage and power performance curves of the GEORBFNN

The DC voltage profile of the proposed photovoltaic/battery system remains stable at 22.1V under varying change in irradiance levels and in the analysis of a load fault, as illustrated in Figure 17.

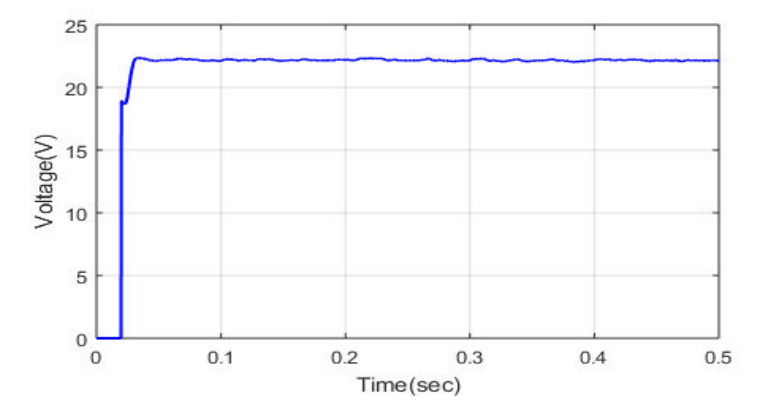


Figure 17: Analysis of Voltage

The results showed that the proposed method outperformed the existing approach in terms of power performance. The proposed method was able to improve the power quality in all tested cases. Figure 18 illustrates the power curves, which depict the changes in irradiance for different components. The power curves for the proposed method include grid power, PV power, battery power, and total power. The grid power flow ranged from 0 to 1200W and remained constant between 0.1 and 0.5 seconds. The PV power flow ranged from 0 to 6000W, was constant at 0.2, then decreased by 3900W, and increased back to 6000W, staying constant thereafter. The battery power flow ranged from 0 to 2200W and remained constant from 0.1 to 0.2 seconds. Finally, the total power flow ranged from 0 to 9700W, stayed constant until 0.2 seconds, reduced to 7500W, and then increased back to 9000W.

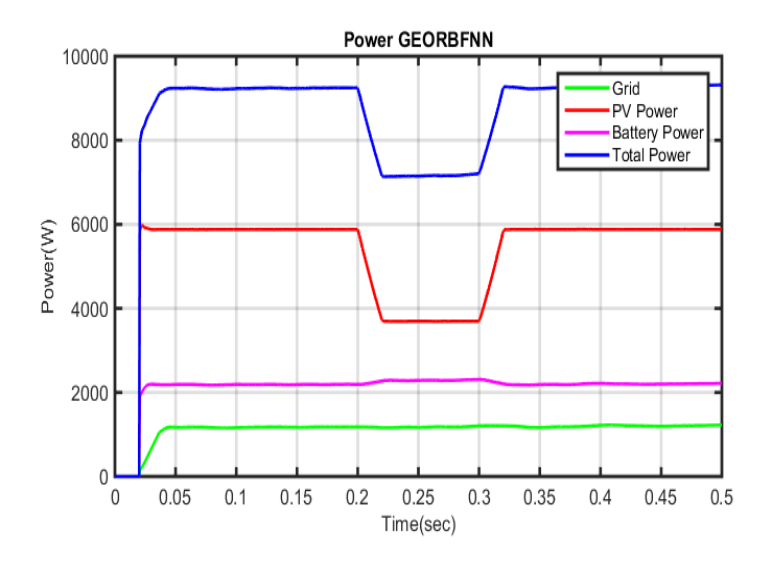


Figure 18: Power Curves of the proposed method for change in irradiance

Figure 19 depicts the power curves for the analysis of load faults. The graph shows the power distribution among the grid, PV system, battery, and total power. The grid power ranges from 0 to 1200W and remains consistent from 0.1 to 0.5 seconds. The PV power ranges from 0 to 6000W and remains constant thereafter. The battery power ranges from 0 to 2200W and stays steady until the end. The total power ranges from 0 to 9700W and remains constant.

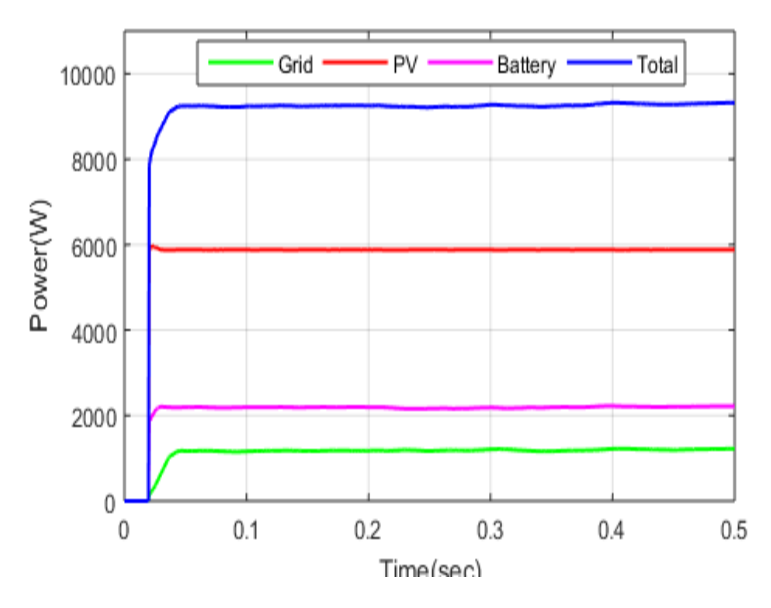


Figure 19: Power Curves of the proposed method for analysis of load fault

6. Conclusion

We can say that we present a GEO-RBFNN method for restoring PQ in a grid-tied hybrid power system that includes photovoltaic storage and batteries, as well as a GDBT-BCMO method for integrating PQ in such a system without changing its conventional scheme of real power transmission. In this case, the RBFNN approach is used to forecast the best control signals, while the GEO method is used to construct the ideal combination of parameters. The BCMO approach is used to create the right mixing parameters, while the GBDT method is used to forecast the optimal control signals. Variables in the system's parameters, such as DC voltage and active/reactive power, make up the prediction process. At this point, we run the suggested technique on the MATLAB/Simulink site and compare its results to those of other methods that are already out there, such as GBDTBCMO, BCMO, ALO, and BAT. To provide the best control signal and keep the GEO-RBFNN's Hybrid Renewable Energy Sources (HRES) running, the suggested solution uses load fluctuation to determine the PI controller gain settings. When compared

to other approaches for GBDT-BCMO, the suggested one produces the best results. The experimental findings show that the GEO-RBFNN approach can handle power quality improvement very well, and when compared to other methods, the suggested result is the best for GEO-RBFNN.

References

- [1] E. Jamil, S. Hameed, B. Jamil and Qurratulain, "Power quality improvement of distribution system with photovoltaic and permanent magnet synchronous generator based renewable energy farm using static synchronous compensator", Sustainable Energy Technologies and Assessments, vol. 35, pp. 98-116, 2019.
- [2] O. Mahela and A. Shaik, "Power quality improvement in distribution network using DSTATCOM with battery energy storage system", International Journal of Electrical Power & Energy Systems, vol. 83, pp. 229-240, 2016.
- [3] M. Ullah and A. Hanif, "Power quality improvement in distribution system using distribution static compensator with super twisting sliding mode control", International Transactions on Electrical Energy Systems, vol. 31, no. 9, 2021.
- [4] S. Agalar and Y. Kaplan, "Power quality improvement using STS and DVR in wind energy system", Renewable Energy, vol. 118, pp. 1031-1040, 2018.
- [5] Janardhan, G., N. N. V. Surendra Babu, and G. N. Srinivas. 2022. "A Hybrid Technique for Transformer-Less Grid-Tie Hybrid Renewable Energy Source with Reduction of Common Mode Leakage Current." *Journal of Intelligent & Fuzzy Systems* 43 (6): 7995–8019. https://doi.org/10.3233/JIFS-213362.
- [6] Jamil, E., S. Hameed, B. Jamil, 2019. "Power Quality Improvement of Distribution System with Photovoltaic and Permanent Magnet Synchronous Generator Based Renewable Energy Farm Using Static Synchronous Compensator." Sustainable Energy Technologies and Assessments 35:98–116. https://doi.org/10.1016/j.seta.2019.06.006.
- [7] Prabhu, Mr. & K., Sundararaju. (2020). Power Quality Improvement of Solar Power Plants in Grid Connected System Using Novel Resilient Direct Unbalanced Control (Rduc) Technique. Microprocessors and Microsystems. 75. 103016. 10.1016/j.micpro.2020.103016.
- [8] Mehta, Gitanjali & Singh, S P. (2013). Power quality improvement through grid integration of renewable energy sources. IETE Journal of Research. 59. 210-218. 10.4103/03772063.2013.10876497.
- [9] Moorthy, V. & S., Siva Subramanian & Tamilselvan, V. & Sankaramoorthy, Muthubalaji & Rajesh, P. & Shajin, Francis. (2022). A hybrid technique-based energy management in hybrid electric vehicle system. International Journal of Energy Research. 46. 10.1002/er.8248.
- [10] Kumari, Naresh. (2020). A hybrid RBFNN–BBMO methodology for robust energy management in grid-Connected microgrid. International Journal of Numerical Modelling: Electronic Networks, Devices and Fields. 33. 10.1002/jnm.2751.
- [11] Vanitha, V. & Vallimurugan, E. (2022). A hybrid approach for optimal energy management system of internet of things enabled residential buildings in smart grid. International Journal of Energy Research. 46. 10.1002/er.8024.
- [12] Shahrabi, E., S. M. Hakimi, A. Hasankhani, G. Derakhshan, and B. Abdi. 2021. "Developing Optimal Energy Management of Energy Hub in the Presence of Stochastic Renewable Energy Resources." Sustainable Energy, Grids and Networks 26:100428. https://doi.org/10.1016/j.segan.2020.100428.
- [13] Khan, M. W., J. Wang, and L. Xiong. 2021. "Optimal Energy Scheduling Strategy for Multi-Energy Generation Grid Using Multi-Agent Systems." International Journal of Electrical Power & Energy Systems 124:106400. https://doi.org/10.1016/j.ijepes.2020.106400.
- [14] Vidhya, K., and K. Krishnamoorthi. 2022. "A Hybrid Technique for Optimal Power Quality Enhancement in Grid-Connected Photovoltaic Interleaved Inverter." Energy & Environment 35 (1): 244–274. https://doi.org/10.1177/0958305X221140574.
- [15] Moghaddam, M. J. H., A. Kalam, J. Shi, S. A. Nowdeh, F. H. Gandoman, and A. Ahmadi. 2020. "A New Model for Reconfiguration and Distributed Generation Allocation in Distribution Network Considering Power Quality Indices and Network Losses." IEEE Systems Journal 14 (3): 3530–3538. https://doi.org/10.1109/ JSYST.2019.2963036.
- [16] Yuvaraj, T., K. R. Devabalaji, N. Prabaharan, H. HaesAlhelou, A. Manju, P. Pal, and P. Siano. 2021. "Optimal Integration of Capacitor and Distributed Generation in Distribution System Considering Load Variation Using Bat Optimization Algorithm." Energies 14 (12): 3548. https://doi.org/10.3390/en14123548.
- [17] D. Thomas, G. D'Hoop, O. Deblecker, K. Genikomsakis and C. Ioakimidis, "An integrated tool for optimal energy scheduling and power quality improvement of a microgrid under multiple demand response schemes", Applied Energy, vol. 260, p. 114314, 2020.